JOURNAL OF GEOPHYSICAL RESEARCH, VOL. 91, NO. B6, PAGES 6535–6545, MAY 10, 1986

Inverse Hydrologic Analysis of the Distribution and Origin of Gulf Coast-Type Geopressured Zones

CRAIG M. BETHKE

Hydrogeology Program, Department of Geology, University of Illinois, Urbana

Inverse hydrologic analysis of compaction-driven groundwater flow provides insights to the distribution and origin of geopressured zones in subsiding sedimentary basins, such as those found in the U.S. Gulf Coast. Occurrences of Gulf Coast-type geopressures are most frequently attributed to "disequilibrium compaction" caused by slow rates of fluid escape from compacting sediments, "aquathermal pressuring" from thermal expansion of pore fluids, or the subsurface dehydration of smectite. This paper presents an inverse solution to the Lagrangian equation of compaction flow that includes effects of aquathermal pressuring and dehydration reactions. The solution gives the permeability profile required to maintain a lithostatic pressure gradient in a subsiding basin. Comparison of the closed-form solution with measured permeabilities shows that geopressured zones are likely to form in shaly basins subsiding more than about 1 mm/yr but unlikely to develop in shale-poor basins or basins subsiding less than 0.1 mm/yr. This result correctly predicts geopressures in the Gulf Coast but suggests that many important sedimentary basins were not significantly overpressured during compaction. Solutions that consider only thermal expansion of pore fluids give required permeabilities about 1.3–1.8 orders of magnitude (factor of 20–60) less than those considering only sediment compaction, indicating that aquathermal pressuring is much less important than disequilibrium compaction in causing geopressures. Solutions accounting for the effects of dehydration reactions show that release of structural water during smectite dehydration can be a significant and perhaps necessary factor in geopressuring. Hydrologic effects of a possible increase in the volume of structural water during dehydration are less significant. The most important contribution of smectite dehydration to development of geopressured zones, however, may be the accompanying reduction of host rock permeability.

INTRODUCTION

Geopressures, pore fluid pressures greatly in excess of hydrostatic, have been observed in sedimentary basins worldwide and have probably been commonplace through geologic time [*Sharp and Domenico*, 1976]. Geopressured zones first attracted attention because of difficulties involved in drilling overpressured formations [*Cannon and Sullins*, 1947; *Dickinson*, 1953; *Thomeer and Bottema*, 1961]. Later workers suggested that geopressures play important roles in localizing petroleum reservoirs [*Fowler*, 1970; *Timko and Fertl*, 1971], forming certain types of ore deposits [*Sharp*, 1978; *Cathles and Smith*, 1983], and controlling sediment deformation and structural development [*Rubey and Hubbert*, 1959; *Bruce*, 1973; *Suppe and Wittke*, 1977; *Engelder and Oertel*, 1985]. Large hydraulic potential gradients associated with geopressured zones can concentrate sedimentry brines by reverse osmosis [*Graf*, 1982] and restrict deep groundwater circulation [*Hanor and Bailey*, 1983]; these zones may represent a future resource of thermal and mechanical energy and dissolved methane [*Wallace et al.*, 1979].

C. A. Stuart coined the term "geopressure" to describe "an overpressure generated by the overburden" [*Parker*, 1974]. Geopressured zones are most often encountered in shaly sections of actively subsiding basins, such as the U.S. Gulf Coast. Fluid pressures in these zones commonly approach the lithostatic limit at which the pore fluid supports the weight of the fluid-saturated overburden. Such occurrences are referred to herein as Gulf Coast-type geopressures. *Bruce* [1973] noted, on the basis of analysis of seismic data, that geopressured shales in the Gulf Coast commonly occur at several kilometers depth, extend for tens of kilometers laterally and are at least several kilometers thick. Conditions at greater depths are poorly known [*Hanor and Bailey*, 1983].

Many authors divide geopressured columns in the Gulf Coast into three sections (Figure 1). Fluid pressures in the lithostatic section approach but do not reach the lithostatic limit [*Dickinson*, 1953]. The lithostatic and overlying hydrostatic sections are separated by a transition interval. Sediment porosity increases across the transition interval and then decreases in the lithostatic section with increasing depth [*Weaver and Beck*, 1971].

The most actively discussed causes of geopressures in Gulf Coast-type settings (review by *Graf* [1982]) are rapid accumulation of fine-grained sediments, "aquathermal pressuring" from thermal expansion of pore fluids, and dehydration reactions of clay minerals. *Dickinson* [1953] interpreted Gulf Coast geopressures to result from the inability of fine-grained sediments to expel pore fluids rapidly enough to accommodate normal gravitational compaction. In this case, sediments cannot compact to their normal or "equilibrium" porosity and are said to be in "disequilibrium compaction" [*Magara*, 1975*a*]. *Barker* [1972] used the term "aquathermal pressuring" to describe the pressure increase due to differential thermal expansion of pore fluids relative to the rock matrix in a subsiding sediment. *Powers* [1967] suggested that geopressures may be generated by the dehydration reaction of smectitic clay minerals forming minerals rich in illite [*Perry and Hower*, 1970, 1972]. This hypothesis is supported by observations that the dehydration reaction occurs at or near the tops of Gulf Coast geopressured zones [*Foster*, 1981; *Berg and Habeck*, 1982; *Bruce*, 1984]. Pressuring by expansion of organics during maturation [*Momper*, 1978] has been less frequently considered.

Parker [1974] differentiates Gulf Coast-type geopressures from those occurring in older, fully compacted strata. A probable cause of the latter in the Mississippi Interior Salt Basin

Paper number 5B5796.
0148-0227/86/005B-5796$05.00

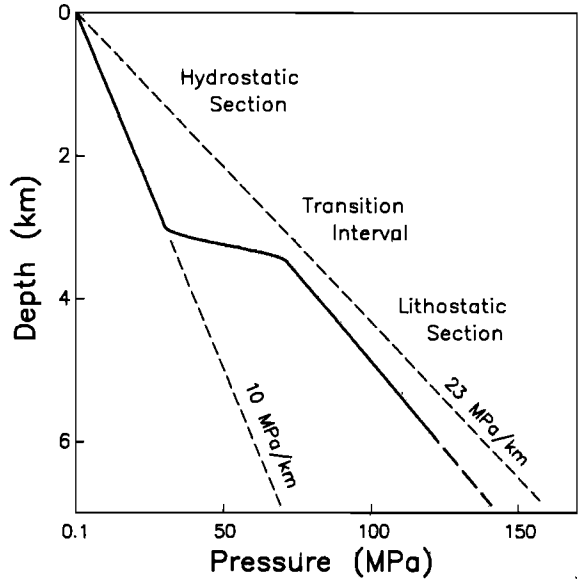

Fig. 1. General trend of fluid pressure versus depth in occurrences of Gulf Coast-type geopressures. Hydrostatically pressured section overlies lithostatic section in which fluid pressures approach the lithostatic limit. Hydrostatic and lithostatic sections are separated by a transition interval, and top of lithostatic section commonly occurs near depth of smectite dehydration reaction.

[*Parker*, 1974] and the Greater Green River Basin [*Law and Dickinson*, 1985] is gas produced by thermal cracking of petroleum and other organics. Additional causes of geopressures, such as lateral tectonic compression [*Berry*, 1973] and topographic relief [*Toth*, 1979] may also be geologically significant but are probably not important in Gulf Coast-type settings. Gypsum dehydration is unlikely to contribute to deep geopressures because the reaction occurs at shallow depths [*Hanshaw and Bredehoeft*, 1968]. *Hubbert and Rubey* [1959], *Tkhostov* [1963], *Hanshaw and Zen* [1965], *Jones* [1969], and *Parker* [1974] further discuss mechanisms of producing excess pressures in the subsurface.

Quantitative study of the nature of Gulf Coast-type geopressures relies upon solving differential equations describing compaction-driven groundwater flow. Recent studies [*Bredehoeft and Hanshaw*, 1968; *Smith*, 1973; *Sharp*, 1976; *Sharp and Domenico*, 1976; *Bethke*, 1985, 1986; *Keith and Rimstidt*, 1985] have used mathematical or numerical modeling techniques to study evolution of pore pressures during basin subsidence. These studies are powerful in their ability to predict pressure distributions resulting from given hydrologic conditions but provide information on the nature of geopressures only indirectly by repeatedly evaluating solutions. *Magara* [1971], however, devised an "inverse modeling" approach in which he solved the compaction flow problem directly for the conditions requisite for geopressuring by assuming a lithostatic pressure gradient as a boundary condition.

This paper extends Magara's work by using inverse techniques to develop an analytical solution to the Lagrangian equation of compaction-driven flow. The solution, which includes effects of aquathermal pressuring and mineral dehydration reactions, gives the permeability profile required to maintain lithostatic pore pressures in sediments during burial. This approach, which predicts permeability values required for geopressuring, allows direct comparison with measured permeabilities to define better the depositional and tectonic environments of Gulf Coast-type geopressured zones in present-day basins as well as basins in the geologic past. The method also permits comparison and ranking by importance of different proposed causes of these geopressures. Improved knowledge of the distribution and origin of geopressures may have important implications in applying current theories in petroleum, economic, and structural geology.

PERMEABILITY EQUATION

To maintain near-lithostatic pressures in a geopressured zone, pore pressures in sediments undergoing burial must continuously increase along an approximately lithostatic gradient. The permeability profile that will result in this increase can be calculated by combining the definition of a lithostatic pressure gradient, observations of porosity versus depth within geopressured zones, and the Lagrangian equation of compaction-driven groundwater flow. Lagrangian coordinates are well suited to the problem because they subside with the sedimentary column during burial and do not require a moving boundary condition at the basement contact. Eulerian coordinates, on the other hand, remain fixed in space but move with respect to the subsiding sediments [*Sharp*, 1983], complicating analysis.

The one-dimensional Lagrangian equation of compaction-driven groundwater flow under polythermal conditions (Appendix A) is

$$\phi\beta \frac{\partial P}{\partial t} = \frac{\partial}{\partial z}\left[\frac{k}{\mu}\left(\frac{\partial P}{\partial z} - \rho g\right)\right] - \frac{1}{(1-\phi)}\frac{\partial \phi}{\partial t} + \phi\alpha \frac{\partial T}{\partial t} + Q_w \tag{1}$$

Mathematical symbols are listed separately in notation section. This equation is derived from Darcy's law for vertical groundwater flow and an equation of state for a pore fluid of constant composition. The equation describes change in pore pressure due to, from left to right, divergence of Darcy fluxes, collapse of pore volume (assuming negligible compressibility of rock grains), thermal expansion of pore fluids, and internal fluid sources.

The pressure gradient and rate of pressure increase in a lithostatically pressured sediment are given as

$$\partial P/\partial z = \rho_{sm} g$$

and

$$\partial P/\partial t = \rho_{sm} g v_z$$

[*Rubey and Hubbert*, 1959]. By substituting these relations into equation (1) and taking porosity and temperature as functions of burial depth, the gradient of the ratio of permeability to viscosity required to maintain lithostatic pore pressures in a sediment during burial is

$$\frac{d}{dz}\left(\frac{k}{\mu}\right) = \frac{v_z}{(\rho_{sm} - \rho)g}\left[\phi\beta\rho_{sm} g + \frac{1}{(1-\phi)}\frac{d\phi}{dz} - \phi\alpha\frac{dT}{dz}\right] + \frac{Q_w}{(\rho_{sm} - \rho)g} \tag{2}$$

This equation accounts, from left to right, for compressive fluid storage, pore volume collapse, fluid thermal expansion, and internal sources of fluid volume.

Equation (2) is an ordinary differential equation of first order that can be solved by integration for the permeability profile of a sedimentary column resting on impermeable basement, given sediment porosity versus depth. Porosity in the

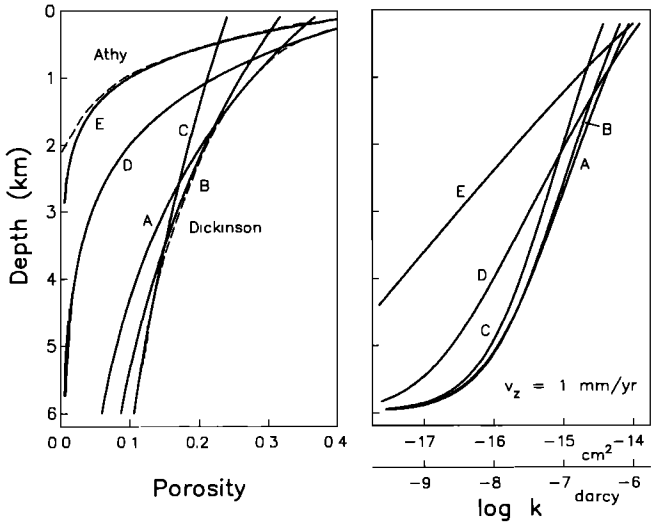

Fig. 2. Permeability k required to maintain lithostatic pore pressures as a function of depth for various porosity profiles (Table 1). Results assume burial at 1 mm/yr but may be adjusted for other burial rates by a factor of v_z. Profiles A–C near Dickinson's fit of Gulf Coast shale porosities give similar results. Profiles D and E closer to Athy's fit to Paleozoic shales in the midcontinent, for comparison, require lesser permeabilities.

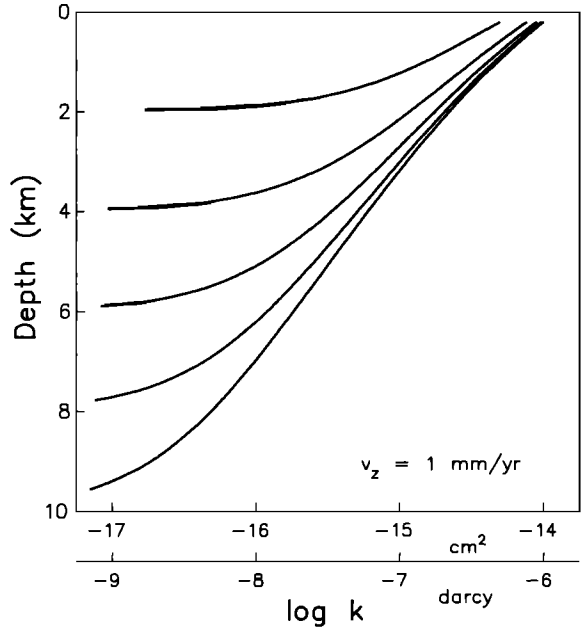

Fig. 3. Permeability profiles required to maintain lithostatic pressures in basins of varying sediment thickness (z_b = 2, 4, 6, 8, and 10 km). Deep basins may develop geopressures in more permeable sediments than shallow basins.

lithostatic section (Figure 1), which decreases gradually as depth increases [*Dickinson*, 1953; *Weaver and Beck*, 1971], is frequently represented by *Athy*'s [1930] law:

$$\phi = \phi_0 e^{-bz} \tag{3}$$

[e.g., *Rubey and Hubbert*, 1959]. Athy's law is a widely accepted description of compaction [*Korvin*, 1984], although *Baldwin and Butler* [1985] favor empirical relations written in terms of solidity, the complement of porosity.

Substituting Athy's law into (2) and integrating upward from an impermeable boundary at z_b gives permeability in the lithostatic section versus depth:

$$k = \frac{v_z \mu}{(\rho_{sm} - \rho)g}\left\{\frac{\alpha(dT/dz) - \beta\rho_{sm}g}{b}[\phi(z) - \phi(z_b)] - b(z_b - z) + \ln\left[\frac{\phi(z)}{\phi(z_b)}\right] + \ln\left[\frac{1-\phi(z_b)}{1-\phi(z)}\right]\right\} - \frac{\mu}{(\rho_{sm} - \rho)g}\int_{z_b}^{z} Q_w\, dz \tag{4}$$

where vertical variation in v_z due to compaction is ignored. Choosing a basal boundary condition allows this equation to be applied anywhere in a lithostatic section resting on basement, regardless of hydrologic conditions in overlying strata.

Equation (4) can be evaluated for any burial rate and coefficients ϕ_0 and b, given appropriate values of α, β, $T(z)$, and μ. Calculations in this paper use α and β values of 7×10^{-4} °C^{-1} and 6×10^{-4} MPa^{-1}, computed from an equation of state for NaCl solutions [*Phillips et al.*, 1981] at the temperature and pressure range of interest. Calculations also assumed a 20°C surface temperature and 25°C/km geothermal gradient, unless noted, and employed the *Mercer et al.* [1975] viscosity correlation with temperature which compares well with data for relatively dilute electrolyte solutions of *Phillips et al.* [1980]. Choice of the Mercer equation is reasonable, because pore fluids from geopressured shales in the Gulf Coast are fairly dilute [*Schmidt*, 1973; *Hanor and Bailey*, 1983], and fluid viscosity is nearly independent of pressure under sedimentary conditions [*Phillips et al.*, 1980].

TABLE 1. Coefficients to Athy's Law Used in Calculations Shown in Figure 2

Profile	ϕ_0	b, cm^{-1}
A[a]	0.38	3.1×10^{-6}
B	0.33	2.2×10^{-6}
C	0.25	1.4×10^{-6}
D	0.50	8.0×10^{-6}
E	0.50	16.0×10^{-6}

[a] *Magara*'s [1971] fit to Dickinson's curve.

Discussion

Evaluating the permeability equation using observed porosity profiles allows analysis of the environments and causes of Gulf Coast-type geopressures. *Hunt* [1979, p. 209] noted that nearly all published porosity profiles fall between curves defined by *Dickinson* [1953] for Tertiary shales of the Gulf Coast and *Athy* [1930] for Paleozoic shales in Oklahoma. Dickinson's curve is representative of young, overpressured sections; Athy's data describe ancient, normally pressured shales.

Figure 2 shows permeability profiles required for geopressuring in a 6-km-deep basin calculated using various porosity profiles falling between Dickinson's and Athy's curves (Table 1). These profiles assume burial at 1 mm/yr, but results can be adjusted for other burial rates by a factor of v_z because k is proportional to v_z in equation (4). Profile A is *Magara*'s [1971] fit to Dickinson's curve. Profiles B and C also fall near Dickinson's curve but have varying slopes. Porosity curves D and E, presented for comparison only, fall closer to Athy's curve representing normally pressured sections and would require lesser permeabilities to maintain geopressures. Inasmuch as porosity profiles A–C near Dickinson's curve give similar permeability profiles, porosity curve A is used in calculations shown in Figures 3–5.

The increase in permeability away from the basal boundary along calculated profiles in Figure 2 arises from the cumulative nature of fluid discharge in a system that has an internal

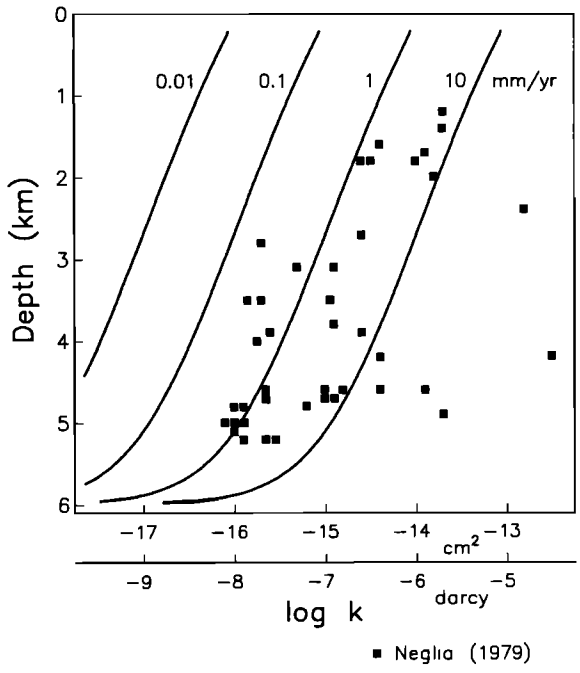

Fig. 4. Permeability profiles calculated for various burial rates, and measured shale permeabilities from Triassic-Pliocene strata [*Neglia*, 1979], obtained by laboratory measurement. To the extent that measurements are representative of permeabilities from Gulf Coast-type basins, geopressures are likely in shaly basins with burial rates greater than 1 mm/yr and unlikely when burial rates of less than 0.1 mm/yr. For comparison, the U.S. Gulf Coast is estimated to contain >85% shaly sediments [*Boles and Franks*, 1979] and is presently subsiding at 1–5 mm/yr [*Holdahl and Morrison*, 1974; *Trahan*, 1982].

pressuring mechanism. Such a hydrologic system has been compared to heat flow in an internally heated medium [*Bethke*, 1985]. In about the lowest half kilometer, calculated permeabilities sharply decrease downward, indicating the difficulty in maintaining a lithostatic pressure gradient near a permeability barrier. Interestingly, fluid pressure gradients seem to flatten out at the base of Gulf Coast geopressured zones [*Hanor and Bailey*, 1983], perhaps because real sediments are unlikely to decrease in permeability in this area as rapidly as equation (4) would require.

Figure 3 gives permeability profiles calculated for differing sediment thicknesses. Thicker sections do not require permeabilities as small as those needed for geopressuring in thinner sections, showing that deeper basins are more easily geopressured. This result, also found by *Magara* [1971], occurs because the total amount of pore volume collapse in a column, and hence the rate of fluid discharge, is greater in a thick than a thin section.

Environments of Gulf Coast-Type Geopressures

The permeability equation can be used to better define the depositional and tectonic environments in which Gulf Coast-type geopressures are likely to occur. Because the analysis presented does not consider the possibility of lateral flow paths of lesser resistance than vertical pathways or hydraulically conductive faults, equation (4) predicts the maximum sediment permeability that could allow geopressuring.

Figure 4 shows equation (4) evaluated for various burial rates of 0.01–10 mm/yr and measured permeabilities of Triassic-Pliocene shales versus depth from *Neglia* [1979]. Burial rates in sedimentary basins rarely exceed 1–10 mm/yr over geologic time periods [*Blatt et al.*, 1980, p. 31]. Neglia's data, obtained by laboratory measurement, span the normal range of 10^{-16}–10^{-12} cm^2 (10^{-8}–10^{-4} darcy) for shale permeabilities [*Freeze and Cherry*, 1979, p. 29], and scatter along a decreasing trend with depth.

Comparison of the solutions and shale permeabilities shows that to the extent that the measured permeabilities are representative of evolving basins, shaly basins that subside at about 1 mm/yr or more rapidly are likely to be geopressured. Geopressuring of even shale-rich basins that subside less than 0.1 mm/yr, however, is improbable. This result agrees with *Bredehoeft and Hanshaw*'s [1968] conclusion that a thick shale section would have to subside at about 0.5 mm/yr to become geopressured. In addition, basins composed primarily of sandstones, limestones, and dolomites are unlikely to develop geopressures during compaction because typical permeabilities of these rock types are 10^{-13}–10^{-9} cm^2 (10^{-5}–10^{-1} darcy) [*Freeze and Cherry*, 1979] well above required permeabilities even at burial rates of 10 mm/yr.

Possible exceptions to the preceding discussion are basins sealed by evaporite beds, such as a northwestern German basin in which Permian strata composed of anhydrite and dolomite overlain by thick halite deposits are geopressured [*Thomeer and Bottema*, 1961]. The few available (review by *Wolff* [1982]) permeability measurements for evaporite rocks (Table 2) span a range of values from not measureable with gas permeant to 1.5×10^{-9} cm^2 (1.5×10^{-1} darcy). Because of limited data and the broad range of reported evaporite permeabilities, quantitative evaluation of the requirements for geopressuring in such basins is difficult. Nonetheless, occurrence of halite samples too impermeable for laboratory

TABLE 2. Permeabilities of Evaporite Rocks by Laboratory Measurement

Rock Type	Number of Measurements	Permeability Range		Reference
		Square Centimeter	Darcy	
Bedded gypsum[a]	4	1.3×10^{-15} to 9.2×10^{-13}	1.3×10^{-7} to 9.3×10^{-5}	*Sanyal et al.* [1971]
Bedded halite	7	0[b] to 2.3×10^{-13}	0[b] to 2.3×10^{-5}	*Gloyna and Reynolds* [1961]
Salt dome halite[c]	19	0[b] to 1.5×10^{-9}	0[b] to 1.5×10^{-1}	*Gloyna and Reynolds* [1961]
Bedded and dome halites[d]	5	1.0×10^{-13} to 7.4×10^{-11}	1.0×10^{-5} to 7.4×10^{-3}	*Aufricht and Howard* [1961]

[a]10.3–12.4 MPa confining pressure.
[b]Not measureable with gas permeant.
[c]Strong dependence of permeability on confining pressure reported.
[d]Gas permeant at 5.5 MPa confining pressure. Permeability decreased as a function of time when a brine permeant was used.

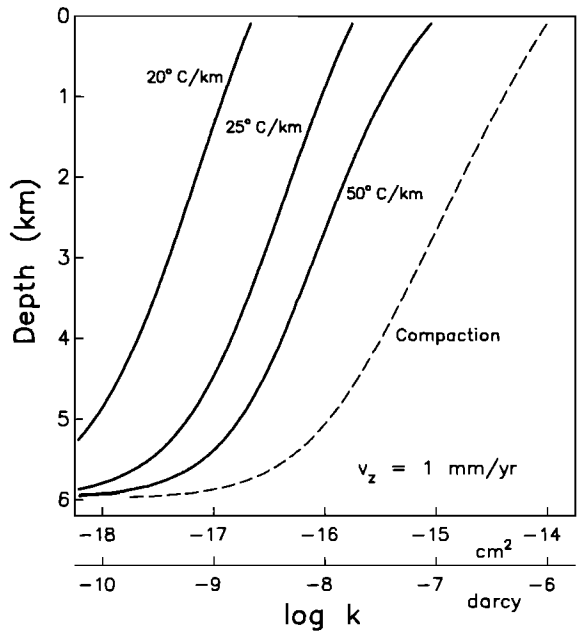

Fig. 5. Solutions to permeability equation considering aquathermal pressuring alone (equation (5)) for various geothermal gradients (solid lines), and considering only compaction (dashed line). Aquathermal pressuring in a basin with a geothermal gradient of 25°C/km requires permeabilities about 1.3–1.8 orders of magnitude less than permeabilities required to maintain lithostatic pressures by sediment compaction alone. Even assuming a geothermal gradient of 50°C/km, the aquathermal solution is about a log unit less than the compaction solution, indicating that aquathermal pressuring is much less important than disequilibrium compaction as a cause of geopressures.

measurement suggests that basins sealed by salt beds might develop geopressures even at relatively small burial rates.

Results in Figure 4 correctly predict geopressures in the U.S. Gulf Coast because this basin contains, by conservative estimate, >85% shales and shaly sediments [*Boles and Franks*, 1979] and is currently subsiding at a natural rate of 1–5 mm/yr [*Holdahl and Morrison*, 1974; *Trahan*, 1982]. This rate may be compared to an estimated range of 0.1–10 mm/yr for Gulf Coast-type basins in general [*Sharp and Domenico*, 1976]. Using these criteria, however, many important sedimentary basins were not significantly overpressured during their compaction. For example, intracratonic basins, such as the Michigan, Illinois, and Williston basins in North America, subside at average rates of only 0.01–0.03 mm/yr [*Schwab*, 1976; *Nalivkin*, 1976], and many interior basins are dominated by carbonate rocks and sandstones rather than shales.

The result that Gulf Coast-type geopressures are only likely to have occurred in a restricted range of tectonic environments may have important implications for petroleum and mineral exploration strategies. Strategies based on current theories relating reservoir localization and ore genesis to geopressured zones might be improved by better prediction of whether target basins have hosted geopressures in the geologic past. Interpretations in structural geology may also be influenced by better understanding of the habitat of Gulf Coast-type geopressures, especially in continental platform and passive margin settings. However, pressuring mechanisms not considered here, such as lateral tectonic compression, may predominate during many types of structural deformation.

Importance of Aquathermal Pressuring

On the basis of analysis of the thermodynamic properties of isolated pore fluids, *Barker* [1972] proposed that geopressured zones in basins that have geothermal gradients greater than about 15°C/km can arise from aquathermal pressuring. Later workers objected to this analysis because pore fluids are not likely to remain truly isolated over geologic time periods. The importance of aquathermal pressuring in contributing to geopressures has been controversial for the past decade [*Magara*, 1975*b*; *Bradley*, 1975; *Domenico and Palciauskas*, 1979; *Chapman*, 1980; *Barker and Horsfield*, 1982; *Chapman*, 1982; *Daines*, 1982; *Sharp*, 1983].

Equation (4), which accounts for migration of pore fluids, can be used to isolate the relative importance of aquathermal effects and compaction in maintaining geopressures. The permeability required for geopressuring by aquathermal effects alone may be derived by taking the limit of equation (4) as b vanishes, giving the constant porosity solution

$$k = \frac{v_z \mu \phi}{(\rho_{sm} - \rho)g}\left(\beta \rho_{sm} g - \alpha \frac{dT}{dz}\right)(z - z_b) \qquad (5)$$

The permeability needed for geopressuring by compaction can be calculated by setting the coefficient of thermal expansion α to zero in (4).

Figure 5 shows permeability profiles required for geopressuring by aquathermal pressuring at geothermal gradients of 20°, 25°, and 50°C/km and a profile calculated considering compaction alone. The solution that considers only compaction gives permeability values about 1.3–1.8 log units (factor of 20–60) greater than those accounting for only aquathermal pressuring at a normal temperature gradient of 25°C/km, which is typical of the Louisiana Gulf Coast [*Barker*, 1972]. Although some geopressured zones have rather large geothermal gradients [*Lewis and Rose*, 1970; *Wallace et al.*, 1979], even calculations assuming a gradient of 50°C/km give permeabilities about an order of magnitude less than the compaction solution. The compaction solution, furthermore, plots on top of the overall solution accounting for both compaction and aquathermal pressuring (Figure 2).

Results in Figure 5 indicate that geopressuring by compaction can be operative in sediments where aquathermal effects alone are insufficient to maintain large excess pressures. In addition, the coincidence of permeability profiles considering compaction alone and compaction plus aquathermal effects argues that aquathermal pressuring does not significantly augment effects of disequlibrium compaction. Thus, although compaction and fluid expansion both generate excess pressures in Gulf Coast-type environments, aquathermal pressuring is clearly the less important cause of geopressures. This result agrees with numerical modeling tests by *Bethke* [1985], which showed that excess pressures only decreased by about 1% when thermal expansion of pore fluids was ignored during simulations of compaction-driven groundwater flow.

Relationship of Smectite Dehydration to Geopressures

Many workers have observed that mixed-layer clay minerals rich in smectite transform diagenetically to illite-rich minerals during burial in sedimentary basins [*Perry and Hower*, 1970, 1972; *Weaver and Beck*, 1971; *Boles and Franks*, 1979]. Although reaction mechanisms in illite-smectite minerals are poorly understood [*Bethke and Altaner*, 1986], structural water within smectite interlayers is released into the sediment pore space during this transformation. *Powers* [1967] proposed that geopressures are caused by this dehydration reaction, and this interpretation has been supported by recent studies that show approximate coincidence of depth intervals of dehydration in the Gulf Coast with the tops of many geo-

TABLE 3. Data Assumed in Calculating Effects of Smectite Dehydration

Parameter	Value	Reference[a]
Fraction illite-smectite in dry sediment	0.6	*Bruce* [1984]
Fraction smectite layers in illite-smectite before reaction	0.8	*Perry and Hower* [1970]
Fraction smectite layers in illite-smectite after reaction	0.2	*Perry and Hower* [1970]
Water layers per smectite layer	2	*Perry and Hower* [1970]
Smectite crystallographic repeat spacing (two water layers)	15 Å	*Burst* [1969]
Dehydrated clay layer thickness	10 Å	*Burst* [1969]

[a]Data based on studies of shales from the U.S. Gulf Coast.

pressured zones [*Foster*, 1981; *Berg and Habeck*, 1982; *Bruce*, 1984].

Smectite dehydration may promote geopressures by releasing interlayer water into pore spaces in the subsurface, possibly accompanied by a volume expansion upon dehydration, as originally envisioned by *Powers* [1967], and by decreasing the permeabilities of host rocks [*Weaver and Beck*, 1971; *Foster*, 1981]. Evaluation of dehydration theories is complicated by poor knowledge of the volumetric properties of interlayer water [*Weaver and Beck*, 1971] and of the fate of the dehydrated water, which may be expelled from the host sediment or accommodated by an increase in pore volume [*Bruce*, 1984]. Nonetheless, effects of dehydration may be explored parametrically to isolate their maximum contributions to geopressures.

This paper makes use of three variables to explore the relationship of smectite dehydration to geopressures. B is a dehydration volume factor that gives the volume of free water produced upon dehydration of a unit volume of interlayer water. Estimates of the value of B (review by *Weaver and Beck* [1971]) range from about 1 [*Burst*, 1969] to 1.4 [*Powers*, 1967]. X is the hydration state of the mineral grains in the host sediment and is defined as the ratio of the volume of structural water to dehydrated minerals. On the basis of data in Table 3, X typically decreases from 0.24 to 0.06 over the course of the dehydration reaction. Finally, Y is a measure of the extra pore volume created to accommodate dehydrated water in a sediment, expressed as a fraction of the cumulative volume of water released within that sediment by a given depth.

These variables can be combined with the analysis presented to isolate hydrologic effects of smectite dehydration from those of the normal gravitational compaction that would occur in the absence of hydrated minerals. Shale porosity is generally calculated from sediment density, derived in the laboratory or from well logs, so that a sediment's measured or "apparent" porosity accounts for the free water comprising "true porosity" as well as interlayer water. From the definition of X, apparent porosity is related to true porosity by

$$\phi = \frac{\phi_t + X}{1 + X} \tag{6}$$

as long as extra pore volume is not created to accommodate dehydrated water ($Y = 0$). Assuming that true porosity varies by Athy's law (equation (3)), the derivative of apparent porosity is

$$\frac{d\phi}{dz} = \frac{1}{(1+X)}\left[\frac{(1-\phi_t)}{(1+X)}\frac{dX}{dz} - b\phi_t\right] \tag{7}$$

Substituting equations (6) and (7) into (2) and accounting for extra fluid volume created by expansion of interlayer water during dehydration as

$$Q_w = (B-1)(1-\phi)\frac{dX}{dz}v_z$$

allows integration using Newton-Cotes quadrature [*Carnahan et al.*, 1969, pp. 69–79] to give permeability versus depth. Appendix B gives expressions for ϕ and $d\phi/dz$ for the more general case in which an arbitrary amount of dehydrated water is accommodated by increased pore space within a sediment.

Figure 6 shows results of integration considering a smectite dehydration reaction occurring as a linear decrease in X downward over a typical depth range of 2.5–3 km [*Bruce*, 1984], assuming negligible fluid volume change ($B = 1$) during dehydration. Values of ϕ_0 and b, describing true porosity, were set at 0.25 and 8×10^{-6} cm^{-1} to approximately match apparent porosity (equation (6)) to Dickinson's curve for Gulf Coast shales. Profile A was calculated assuming that all dehydrated water is lost immediately to the sediment ($Y = 0$); profile B considers gradual loss of all dehydrated water; and C assumes a 50% loss with depth, by z_b. In the latter profiles, Y decreased linearly from one at 2.5 km depth to zero or 0.5 at z_b. For comparison, the dashed line shows the permeability required for geopressuring when no hydrated minerals are present in the sediment at deposition, calculated by setting X to zero. The profile calculated assuming retention of all dehy-

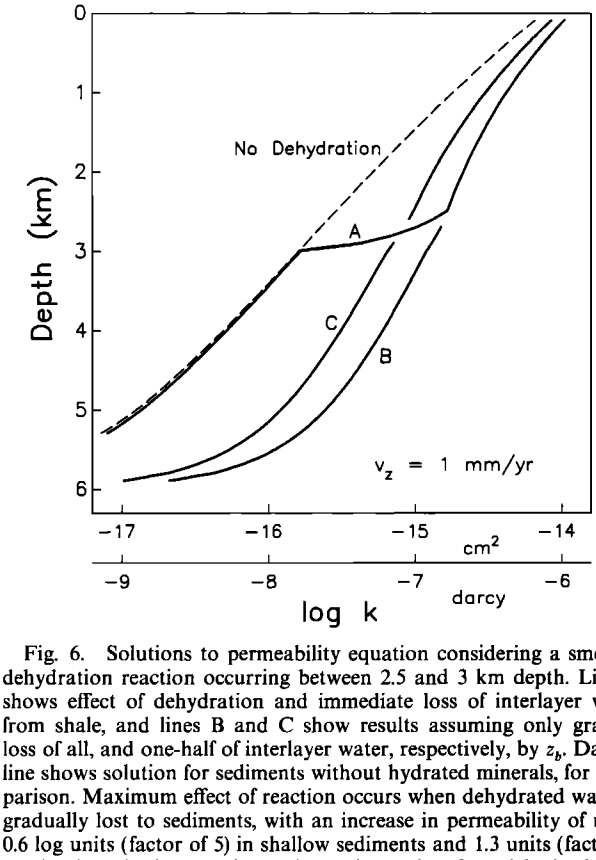

Fig. 6. Solutions to permeability equation considering a smectite dehydration reaction occurring between 2.5 and 3 km depth. Line A shows effect of dehydration and immediate loss of interlayer water from shale, and lines B and C show results assuming only gradual loss of all, and one-half of interlayer water, respectively, by z_b. Dashed line shows solution for sediments without hydrated minerals, for comparison. Maximum effect of reaction occurs when dehydrated water is gradually lost to sediments, with an increase in permeability of up to 0.6 log units (factor of 5) in shallow sediments and 1.3 units (factor of 20) in deep basin. Results indicate that subsurface dehydration of smectite can be a significant and perhaps necessary cause of geopressures.

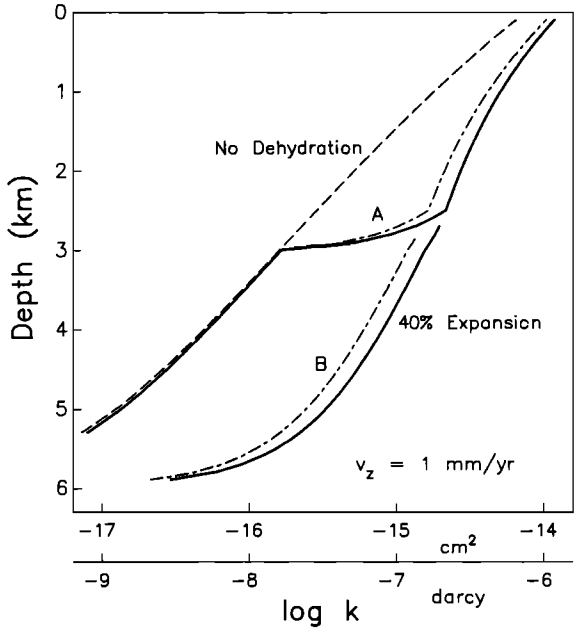

Fig. 7. Solutions to permeability equation considering smectite dehydration between 2.5 and 3 km depth and taking into account possible volume change of interlayer water upon dehydration. A 40% expansion, the maximum suggested by previous authors, shifts curves A and B from Figure 6 (patterned lines) to permeability values increased by as much as 35% (solid lines). This shift is small relative to results in Figure 6, arguing that release of interlayer water at depth is more important than expansion during dehydration in promoting geopressures.

drated water to z_b ($Y = 1$) plots nearly on top of the dashed line and is not shown.

Results in Figure 6 show that smectite dehydration can allow sediments with significantly greater permeabilities than would be required in the absence of such a reaction to be geopressured. Profile A, calculated assuming that pore volume is not increased during dehydration, shows increased likelihood of geopressuring above, but not below the dehydration interval, counter to most geologic observations. Profiles B and C, in which pore volume increases to hold dehydrated water and then decreases gradually as depth increases, however, predict a positive shift of as much as 1.3 log units (factor of 20), relative to the profile for no dehydration, at depths below the reaction interval. These latter profiles, which seem reasonable geologically because sediment porosities in the Gulf Coast increase across the reaction interval and then decrease as depth increases, better match observations that the dehydration interval lies near the tops of geopressured zones in basins worldwide [*Bruce*, 1984].

Figure 7 shows the added effects of a 40% expansion of interlayer water during dehydration ($B = 1.4$), the largest expansion suggested by previous authors. Expansion of interlayer water shifts profile A in the area above the reaction interval to permeabilities <30% greater than those shown in Figure 6 but has no effect at depths below the reaction. Expansion can promote geopressures below the reaction interval if dehydrated water is accommodated by increased pore volume, as shown by the shift of profile B. The magnitude of this shift, however, is <35%, arguing that the possible volume change of interlayer water during smectite dehydration is secondary to the release of interlayer water at depth as a cause of geopressures.

The dehydration reaction of smectite, then, can promote geopressuring if interlayer water is retained in sediments after dehydration and gradually lost during further burial by compaction. Calculations of the efficacy of this reaction in causing geopressures suggest that under optimum conditions, basins filled with sediments rich in smectite can become overpressured at permeabilities about twenty times greater or burial rates 20 times less than basins poor in hydrated minerals. Although this result is sensitive to partitioning of true from interlayer porosity, its magnitude compared to results in Figure 4 raises the possibility that smectite dehydration is necessary for geopressuring even at the high burial rates typical of the Gulf Coast.

The ability of smectite to carry water into the subsurface, however, may be somewhat less important in causing geopressures than its capacity to decrease the permeability of host rocks during dehydration. Figure 8 shows shale permeabilities versus depth that *Foster* [1981] estimated for a Gulf Coast well from drilling and well log data. Permeability values decrease sharply across the reaction interval of smectite dehydration by 1.5–2 log units (factor of 30–100). Foster tentatively attributed this permeability drop to silica cementation resulting from smectite illitization, as described by *Towe* [1962] and *Boles and Franks* [1979]. To the extent that these data are representative of shales undergoing smectite dehydration, the reduction in host rock permeability (Figure 8) is of greater magnitude than the calculated effects of water release (Figures 6–7) accompanying this reaction. Results of this study, then, support interpretations by *Weaver and Beck* [1971] and *Foster* [1981] that the single greatest factor in the observed association of smectite dehydration with geopressures is the sealing effect of the reaction on host shales.

CONCLUSIONS

Analysis of compaction-driven groundwater flow provides important insights about the depositional and tectonic envi-

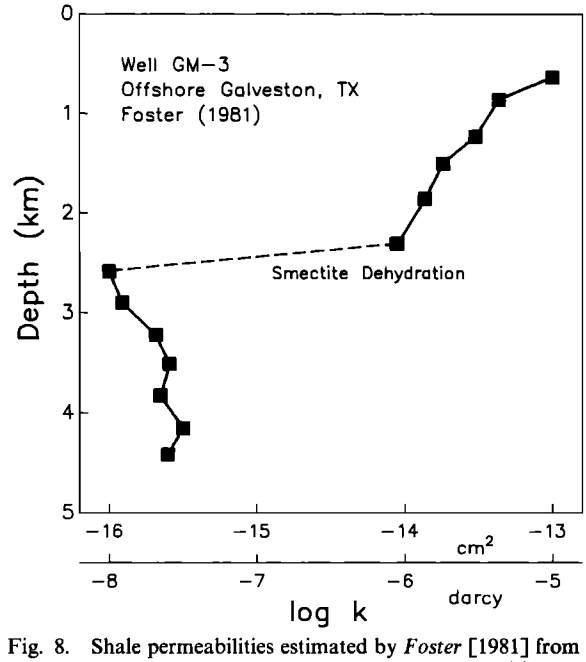

Fig. 8. Shale permeabilities estimated by *Foster* [1981] from drilling and well log data for a Gulf Coast well. Permeabilities decrease sharply across the depth at which smectite dehydration occurs. This decrease of 1.5–2 orders of magnitude (factor of 30–100) suggests that the most important reason for association of the dehydration reaction with tops of geopressured zones may be the sealing effect of illitized shales, as suggested by *Weaver and Beck* [1971] and *Foster* [1981].

ronments in which Gulf Coast-type geopressures are likely to develop, as well as the causes of geopressures. Comparing calculated permeabilities needed to maintain lithostatic pressures in a basin with measured permeabilities of sedimentary rocks shows that shaly basins that have burial rates of at least 1 mm/yr are likely to become geopressured. Shaly basins with burial rates of <0.1 mm/yr and basins dominated by carbonate rocks or sandstones, however, are unlikely to develop significant overpressures during compaction. Burial rates required for geopressuring in basins rich in evaporite beds are difficult to predict because of poor knowledge of evaporite permeabilities.

Using these criteria, geopressuring is predicted for the U.S. Gulf Coast, which is estimated to contain >85% shale and is subsiding at 1–5 mm/yr. Intracratonic basins, on the other hand, are often shale-poor and typically subside at 0.01–0.03 mm/yr, indicating that geopressuring during compaction of these basins is unlikely. These results suggest that exploration strategies based on theories relating localization of petroleum reservoirs and ore deposits by past geopressures should account for lithologies and former burial rates in target basins. Structural interpretations based on the roles of pore pressures in sediment deformation may also be affected by the predicted habitat of geopressures.

Additional calculations isolating the effects of thermal expansion of pore fluids and sediment compaction in producing geopressures allow evaluation of the controversial theory of aquathermal pressuring [*Barker*, 1972]. Although both thermal expansion and compaction generate excess pressures, aquathermal pressuring alone is much less important than observed sediment compaction in causing Gulf Coast-type geopressured zones. Aquathermal pressuring is further found not to significantly augment effects of compaction in producing excess pressures. For these reasons, the theory of disequilibrium compaction [*Dickinson*, 1953] better describes the origin of Gulf Coast-type geopressures than the theory of aquathermal pressuring.

The nature of the relationship of smectite dehydration to the occurrence of geopressured zones in compacting basins may be evaluated by further refinement of this analysis. Calculations show that release of interlayer water at depth can be a significant and perhaps necessary factor in causing geopressures. Hydrologic effects of the possible expansion of structural water upon dehydration are less significant than the effects of water release at depth. These effects combined, however, may not be as important as the decrease in shale permeability that, based on limited data, occurs during the dehydration reaction. Although further measurements of shale permeabilities before and after dehydration are needed to verify this result, calculations support the interpretation of *Weaver and Beck* [1971] and *Foster* [1981] that the most significant role of smectite dehydration in producing geopressures is the sealing of host rocks, possibly by silica cementation of pore spaces.

APPENDIX A: LAGRANGIAN EQUATION OF COMPACTION FLOW

Groundwater flow in a compacting medium undergoing burial through a geothermal gradient can be described by a differential equation in Lagrangian coordinates [*Bethke*, 1985]. The Lagrangian equation is derived by considering an elemental control volume [*Freeze and Cherry*, 1979, pp. 63–69] that always contains the same rock grains. A pore fluid of constant composition within the elemental volume behaves according to a thermodynamic equation of state

$$\frac{1}{\rho}\frac{\partial \rho}{\partial t} = \beta \frac{\partial P}{\partial t} - \alpha \frac{\partial T}{\partial t} \tag{A1}$$

[*Domenico and Palciauskas*, 1979; *Lewis and Randall*, 1961]. The definitions of density and porosity give

$$\frac{\partial \rho}{\partial t} = \frac{1}{V}\frac{\partial m}{\partial t} - \frac{\rho}{V}\frac{\partial V}{\partial t} \tag{A2}$$

and, if compression of rock grains is negligible,

$$\frac{\partial V}{\partial t} = \frac{V_b}{(1-\phi)}\frac{\partial \phi}{\partial t} \tag{A3}$$

From Darcy's law,

$$q = -\frac{k}{\mu}\left(\frac{\partial P}{\partial z} - \rho g\right)$$

[*Bear*, 1972], which gives fluid specific discharge relative to the subsiding medium, the rate of accumulation of fluid mass within the elemental volume can be written

$$\frac{1}{V_b}\frac{\partial m}{\partial t} = -\frac{\partial}{\partial z}(\rho q) + \rho Q_w \simeq \rho \frac{\partial}{\partial z}\left[\frac{k}{\mu}\left(\frac{\partial P}{\partial z} - \rho g\right)\right] + \rho Q_w \tag{A4}$$

where Q_w is the rate of fluid volume addition from an internal source, such as expansion of structural water. Combining equation (A1) with relations (A2)–(A4) gives the compaction flow equation

$$\phi\beta \frac{\partial P}{\partial t} = \frac{\partial}{\partial z}\left[\frac{k}{\mu}\left(\frac{\partial P}{\partial z} - \rho g\right)\right] - \frac{1}{(1-\phi)}\frac{\partial \phi}{\partial t} + \phi\alpha \frac{\partial T}{\partial t} + Q_w$$

From left to right, terms on the right side of this equation describe variation in pore pressure due to divergence of Darcy fluxes, collapse of pore volume, thermal expansion of pore fluids, and internal volume sources.

APPENDIX B: GENERAL DESCRIPTION OF POROSITY EVOLUTION

Porosity in a subsiding sediment undergoing a dehydration reaction can be described in general terms to explore parametrically the relationship of smectite dehydration to geopressures. The following development describes porosity evolution in terms of the hydration state of the minerals grains, X; the dehydration volume factor, B; and the ratio of the volume of dehydrated water accommodated in the sediment to the cummulative volume of water dehydrated within the sediment by a given depth, Y.

In general, the apparent porosity of a sediment is the ratio of the sum of the pore volume expected during compaction ignoring mineral dehydration (V_p), the volume of interlayer water (V_i), and the additional pore volume that might be created to accommodate dehydrated water (V_d), to bulk volume

$$\phi = \frac{V_p + V_i + V_d}{V_p + V_i + V_d + V_g} \tag{B1}$$

X is defined as the ratio of interlayer to mineral grain volumes,

$$X = \frac{V_i}{V_g} \tag{B2}$$

The volume of dehydrated water accommodated by increased porosity of the sediment is given by the product of the fraction of dehydrated water retained, its dehydration volume factor, and the hydration state relative to the initial hydration state of the sediment, X_0,

$$\frac{V_d}{V_g} = BY(X_0 - X) \tag{B3}$$

Finally, the definition of true porosity (equation (6)) can be rearranged to give

$$\frac{V_p}{V_g} = \frac{\phi_t(1 + X)}{(1 - \phi_t)} \tag{B4}$$

Substituting equations (B2)–(B4) into (B1) gives the general porosity relation

$$\phi = \frac{\phi_t + X + BY(X_0 - X)(1 - \phi_t)}{1 + X + BY(X_0 - X)(1 - \phi_t)} \tag{B5}$$

which can be used in evaluating equation (2). The porosity derivative in (2) may be calculated as

$$\frac{\partial \phi}{\partial z} = \frac{1}{v}\frac{\partial u}{\partial z} - \frac{\phi}{v}\frac{\partial v}{\partial z}$$

where u and v are the numerator and denominator of equation (B5) and

$$\frac{\partial u}{\partial z} = b[BY(X_0 - X) - 1]\phi_t + [1 - BY(1 - \phi_t)]\frac{\partial X}{\partial z} + B(X_0 - X)(1 - \phi_t)\frac{\partial Y}{\partial z}$$

$$\frac{\partial v}{\partial z} = [1 - BY(1 - \phi_t)]\frac{\partial X}{\partial z} + B(X_0 - X)(1 - \phi_t)\frac{\partial Y}{\partial z} + b\,BY(X_0 - X)\,\phi_t$$

NOTATION

- b exponential factor in Athy's law (L^{-1}).
- B dehydration volume factor, ratio of dehydrated to hydrated water volumes.
- g acceleration of gravity (L/t^2).
- k vertical intrinsic permeability (L^2).
- m fluid mass within an elemental control volume (M).
- P pore fluid pressure (M/Lt^2).
- q fluid specific discharge (L/t).
- Q_w internal source rate of fluid volume per unit bulk volume (t^{-1}).
- t time (t).
- T temperature (T).
- u numerator of equation (B5).
- v denominator of equation (B5).
- v_z burial rate (L/t).
- V fluid volume in an elemental control volume (L^3).
- V_b bulk volume of an elemental control volume (L^3).
- V_d extra pore volume created in a sediment to accommodate mineral dehydration (L^3).
- V_g volume of rock grains, excluding interlayer water (L^3).
- V_i volume of interlayer water (L^3).
- V_p volume of free pore fluid, excluding dehydrated water (L^3).
- X hydration state of rock grains, V_i/V_g.
- X_0 initial hydration state of sediment.
- Y ratio of V_d to cumulative volume of water released by mineral dehydration reactions by a given depth in a sediment, equal to $V_d/B(X_0 - X)V_g$.
- z burial depth (L).
- z_b depth to impermeable basement (L).
- α isobaric coefficient of thermal expansion for pore fluid (T^{-1}).
- β isothermal coefficient of compressibility for pore fluid (Lt^2/M).
- μ fluid dynamic viscosity (M/Lt).
- ϕ sediment "apparent" porosity, accounting for all fluid volume.
- ϕ_0 preexponential factor in Athy's law.
- ϕ_t sediment "true" porosity, accounting for free pore fluid and excluding interlayer water.
- ρ fluid density (M/L^3), taken as 1.0 g/cm^3.
- ρ_{sm} density of fluid-saturated medium (M/L^3), taken as 2.3 g/cm^3.

L, length; t, time; M, mass; T, temperature.

Acknowledgments. This research was sponsored by Exxon Production Research Company, ARCO Resources Technology Company, and the University of Illinois Research Board. W. R. Foster of Mobil Research and Development Corporation kindly provided data from his 1981 technical presentation. Karolyn Roberts typed the manuscript; Gretchen Goeckner and Mindy James helped edit it. I thank two anonymous colleagues for thoughtful reviews.

REFERENCES

Athy, L. F., Density, porosity, and compaction of sedimentary rocks, *Am. Assoc. Pet. Geol. Bull.*, *14*, 1–24, 1930.

Aufricht, W. R., and K. C. Howard, Salt characteristics as they affect storage of hydrocarbons, *J. Pet. Technol.*, *13*, 733–738, 1961.

Baldwin, B., and C. O. Butler, Compaction curves, *Am. Assoc. Pet. Geol. Bull.*, *69*, 622–626, 1985.

Barker, C., Aquathermal pressuring—Role of temperature in development of abnormal pressure zones, *Am. Assoc. Pet. Geol. Bull.*, *56*, 2068–2071, 1972.

Barker, C., and B. Horsfield, Mechanical versus thermal cause of abnormally high pore pressures in shales: Discussion, *Am. Assoc. Pet. Geol. Bull.*, *66*, 99–100, 1982.

Bear, J., *Dynamics of Fluids in Porous Media*, 764 pp., Elsevier, New York, 1972.

Berg, R. R., and M. F. Habeck, Abnormal pressures in the lower Vicksburg, McAllen Ranch field, South Texas, *Trans. Gulf Coast Assoc. Geol. Soc.*, *32*, 247–253, 1982.

Berry, F. A. F., High fluid potentials in California Coast Ranges and their tectonic significance, *Am. Assoc. Pet. Geol. Bull.*, *57*, 1219–1249, 1973.

Bethke, C. M., A numerical model of compaction-driven groundwater flow and heat transfer and its application to the paleohydrology of intracratonic sedimentary basins, *J. Geophys. Res.*, *90*, 6817–6828, 1985.

Bethke, C. M., Hydrologic constraints on genesis of the Upper Mississippi Valley Mineral District from Illinois Basin brines, *Econ. Geol.*, *81*, 233–249, 1986.

Bethke, C. M., and S. P. Altaner, Layer-by-layer mechanism of smectite illitization and application to a new rate law, *Clays Clay Miner.*, *34*, 136–145, 1986.

Blatt, H., G. Middleton, and R. Murray, *Origin of Sedimentary Rocks*, 2nd ed., 782 pp., Prentice-Hall, Englewood Cliffs, N. J., 1980.

Boles, J. R., and S. G. Franks, Clay diagenesis in Wilcox sandstones of southwest Texas: Implications of smectite diagenesis on sandstone cementation, *J. Sediment. Petrol.*, *49*, 55–70, 1979.

Bradley, J. S., Abnormal formation pressure, *Am. Assoc. Pet. Geol. Bull.*, *59*, 957–973, 1975.

Bredehoeft, J. D., and B. B. Hanshaw, On the maintenance of anomalous fluid pressures, I, Thick sedimentary sequences, *Geol. Soc. Am. Bull.*, *79*, 1097–1106, 1968.

Bruce, C. H., Pressured shale and related sediment deformation: Mechanism for development of regional contemporaneous faults, *Am. Assoc. Pet. Geol. Bull.*, *57*, 878–886, 1973.

Bruce, C. H., Smectite dehydration—Its relation to structural devel-

opment and hydrocarbon accumulation in the northern Gulf of Mexico Basin, *Am. Assoc. Pet. Geol. Bull., 68*, 673–683, 1984.

Burst, J. F., Diagenesis of Gulf Coast clayey sediments and its possible relation to petroleum migration, *Am. Assoc. Pet. Geol. Bull., 53*, 73–93, 1969.

Cannon, G. E., and R. S. Sullins, Problems encountered in drilling abnormal pressure formations, in *Drilling and Production Practice 1946*, pp. 29–33, American Petroleum Institute, Baltimore, Md., 1947.

Carnahan, B., H. A. Luther, and J. O. Wilkes, *Applied Numerical Methods*, 604 pp., John Wiley, New York, 1969.

Cathles, L. M., and A. T. Smith, Thermal constraints on the formation of Mississippi Valley-type lead-zinc deposits and their implications for episodic basin dewatering and deposit genesis, *Econ. Geol., 78*, 983–1002, 1983.

Chapman, R. E., Mechanical versus thermal cause of abnormally high pore pressures in shales, *Am. Assoc. Pet. Geol. Bull., 64*, 2179–2183, 1980.

Chapman, R. E., Mechanical versus thermal cause of abnormally high pore pressures in shales: Reply, *Am. Assoc. Pet. Geol. Bull., 66*, 101–102, 1982.

Daines, S. R., Aquathermal pressuring and geopressure evaluation, *Am. Assoc. Pet. Geol. Bull., 66*, 931–939, 1982.

Dickinson, G., Geological aspects of abnormal reservoir pressures in Gulf Coast Louisiana, *Am. Assoc. Pet. Geol. Bull., 37*, 410–432, 1953.

Domenico, P. A., and V. V. Palciauskas, Thermal expansion of fluids and fracture initiation in compacting sediments, *Geol. Soc. Am. Bull., 90, Part II*, 953–979, 1979.

Engelder, T., and G. Oertel, Correlation between abnormal pore pressure and tectonic jointing in the Devonian Catskill Delta, *Geology, 13*, 863–866, 1985.

Foster, W. R., The smectite-illite transformation: Its role in generating and maintaining geopressure (abstract), *Geol. Soc. Am. Abstr. Programs, 94*, 454, 1981.

Fowler, W. A., Pressures, hydrocarbon accumulation, and salinities—Chocolate Bayou Field, Brazoria County, Texas, *J. Pet. Technol., 22*, 411–423, 1970.

Freeze, R. A., and J. A. Cherry, *Groundwater*, 604 pp., Prentice-Hall, Englewood Cliffs, N. J., 1979.

Gloyna, E. F., and T. D. Reynolds, Permeability measurements of rock salt, *J. Geophys. Res., 66*, 3913–3921, 1961.

Graf, D. L., Chemical osmosis, reverse chemical osmosis, and the origin of subsurface brines, *Geochim. Cosmochim. Acta, 46*, 1431–1448, 1982.

Hanor, J. S., and J. E. Bailey, Use of hydraulic head and hydraulic gradient to characterize geopressured sediments and the direction of fluid migration in the Louisiana Gulf Coast, *Trans. Gulf Coast Assoc. Geol. Soc., 33*, 115–122, 1983.

Hanshaw, B. B., and J. D. Bredehoeft, On the maintenance of anomalous fluid pressures, II, Source layer at depth, *Geol. Soc. Am. Bull., 79*, 1107–1122, 1968.

Hanshaw, B. B., and E. Zen, Osmotic equilibrium and overthrust faulting, *Geol. Soc. Am. Bull., 76*, 1379–1385, 1965.

Holdahl, S. R., and N. L. Morrison, Regional investigations of vertical crustal movements in the U.S., using precise relevelings and mareograph data, *Tectonophysics, 23*, 373–390, 1974.

Hubbert, M. K., and W. W. Rubey, Mechanics of fluid filled porous solids and its application to overthrust faulting, 1, Role of fluid pressure in mechanics of overthrust faulting, *Geol. Soc. Am. Bull., 70*, 115–166, 1959.

Hunt, J. M., *Petroleum Geochemistry and Geology*, 617 pp., W. H. Freeman, San Francisco, Calif., 1979.

Jones, P. H., Hydrodynamics of geopressure in the northern Gulf of Mexico Basin, *J. Pet. Technol., 21*, 803–810, 1969.

Keith, L. A., and J. D. Rimstidt, A numerical compaction model of overpressuring in shales, *Math. Geol., 17*, 115–135, 1985.

Korvin, G., Shale compaction and statistical physics, *Geophys. J. R. Astron. Soc., 78*, 35–50, 1984.

Law, B. E., and W. W. Dickinson, Conceptual model for origin of abnormally pressured gas accumulations in low-permeability reservoirs, *Am. Assoc. Pet. Geol. Bull., 69*, 1295–1304, 1985.

Lewis, C. R., and S. C. Rose, A theory relating high temperatures and overpressures, *J. Pet. Technol., 22*, 11–16, 1970.

Lewis, G. N., and M. Randall, *Thermodynamics*, 2nd ed., revised by K. S. Pitzer and L. Brewer, 723 pp., McGraw-Hill, New York, 1961.

Magara, K., Permeability considerations in generation of abnormal pressures, *Soc. Pet. Eng. J., 11*, 236–242, 1971.

Magara, K., Reevaluation of montmorillonite dehydration as cause of abnormal pressure and hydrocarbon migration, *Am. Assoc. Pet. Geol. Bull., 59*, 292–302, 1975*a*.

Magara, K., Importance of aquathermal pressuring effect in Gulf Coast, *Am. Assoc. Pet. Geol. Bull., 59*, 2037–2045, 1975*b*.

Mercer, J. W., G. F. Pinder, and I. G. Donaldson, A Galerkin–finite element analysis of the hydrothermal system at Wairakei, New Zealand, *J. Geophys. Res., 80*, 2608–2621, 1975.

Momper, J. A., Oil migration limitations suggested by geological and geochemical considerations, in *Physical and Chemical Constraints on Petroleum Migration, Continuing Educ. Course Note Ser.*, vol. 8, pp. B1–B60, American Association of Petroleum Geologists, Tulsa, Okla., 1978.

Nalivkin, V. D., Dynamics of the development of the Russian platform structures, *Tectonophysics, 36*, 247–262, 1976.

Neglia, S., Migration of fluids in sedimentary basins, *Am. Assoc. Pet. Geol. Bull., 63*, 573–597, 1979.

Parker, C. A., Geopressures and secondary porosity in the deep Jurassic of Mississippi, *Trans. Gulf Coast Assoc. Geol. Soc., 24*, 69–80, 1974.

Perry, E., and J. Hower, Burial diagenesis in Gulf Coast pelitic sediments, *Clays Clay Miner., 18*, 165–177, 1970.

Perry, E. A., Jr., and J. Hower, Late-stage dehydration in deeply buried pelitic sediments, *Am. Assoc. Pet. Geol. Bull., 56*, 2013–2021, 1972.

Phillips, S. L., H. Ozbek, A. Igbene, and G. Litton, Viscosity of NaCl and other solutions up to 350°C and 50 MPa pressures, *Lawrence Berkeley Lab. Rep., LBL-11586*, 71 pp., 1980.

Phillips, S. L., A. Igbene, J. A. Fair, H. Ozbek, and M. Tavana, A technical databook for geothermal energy utilization, *Lawrence Berkeley Lab. Rep., LBL-12810*, 46 pp., 1981.

Powers, M. C., Fluid-release mechanisms in compacting marine mudrocks and their importance in oil exploration, *Am. Assoc. Pet. Geol. Bull., 51*, 1240–1254, 1967.

Rubey, W. W., and M. K. Hubbert, Overthrust belt in geosynclinal area of western Wyoming in light of fluid-pressure hypothesis, 2, Role of fluid pressure in mechanics of overthrust faulting, *Geol. Soc. Am. Bull., 70*, 167–205, 1959.

Sanyal, S. K., K. A. Kvenvolden, and S. S. Marsden, Jr., Permeabilities of Precambrian Onverwacht cherts and other low permeability rocks, *Nature, 232*, 325–327, 1971.

Schmidt, G. W., Interstitial water composition and geochemistry of deep Gulf Coast shales and sandstones, *Am. Assoc. Pet. Geol. Bull., 57*, 321–337, 1973.

Schwab, F. L., Modern and ancient sedimentary basins: Comparative accumulation rates, *Geology, 4*, 723–727, 1976.

Sharp, J. M., Jr., Momentum and energy balance equations for compacting sediments, *Math. Geol., 8*, 305–322, 1976.

Sharp, J. M., Jr., Energy and momentum transport model of the Ouachita Basin and its possible impact on formation of economic mineral deposits, *Econ. Geol., 73*, 1057–1068, 1978.

Sharp, J. M., Jr., Permeability controls on aquathermal pressuring, *Am. Assoc. Pet. Geol. Bull., 67*, 2057–2061, 1983.

Sharp, J. M., Jr., and P. A. Domenico, Energy transport in thick sequences of compacting sediment, *Geol. Soc. Am. Bull., 87*, 390–400, 1976.

Smith, J. E., Shale compaction, *Soc. Pet. Eng. J., 13*, 12–22, 1973.

Suppe, J., and J. H. Wittke, Abnormal pore-fluid pressures in relation to stratigraphy and structure in the active fold-and-thrust belt of northwestern Taiwan, *Pet. Geol. Taiwan, 14*, 11–24, 1977.

Thomeer, J. H. M. A., and J. A. Bottema, Increasing occurrence of abnormally high reservoir pressures in boreholes, and drilling problems resulting therefrom, *Am. Assoc. Pet. Geol. Bull., 45*, 1721–1730, 1961.

Timko, D. J., and W. H. Fertl, Relationship between hydrocarbon accumulation and geopressure and its economic significance, *J. Pet. Technol., 23*, 923–933, 1971.

Tkhostov, B. A., *Initial Rock Pressures in Oil and Gas Deposits*, 118 pp., Macmillan, New York, 1963.

Toth, J., Patterns of dynamic pressure increment of formation-fluid flow in large drainage basins, exemplified by the Red Earth region, Alberta, Canada *Bull. Can. Pet. Geol., 27*, 63–86, 1979.

Towe, K. M., Clay mineral diagenesis as a possible source of silica cement in sedimentary rocks, *J. Sediment. Petrol., 32*, 26–28, 1962.

Trahan, D. B., Monitoring local subsidence in areas of potential geopressured fluid withdrawal, southwestern Louisiana, *Trans. Gulf Coast Assoc. Geol. Soc.*, *32*, 231–236, 1982.

Wallace, R. H., Jr., T. F. Kraemer, R. E. Taylor, and J. B. Wesselman, Assessment of geopressured-geothermal resources in the northern Gulf of Mexico Basin, *U.S. Geol. Surv. Circ.*, *790*, 132–155, 1979.

Weaver, C. E., and K. C. Beck, Clay water diagenesis during burial: How mud becomes gneiss, *Spec. Pap. Geol. Soc. Am.*, *134*, 96 pp., 1971.

Wolff, R. G., Physical properties of rocks—Porosity, permeability, distribution coefficients, and dispersivity, *U.S. Geol. Surv. Open File Rep.*, *82-166*, 118 pp., 1982.

C. M. Bethke, Hydrogeology Program, Department of Geology, University of Illinois, 1301 West Green Street, Urbana, IL 61801.

(Received September 5, 1985;
revised January 2, 1986;
accepted January 28, 1986.)